Available online at www.sciencedirect.com
ScienceDirect
Icarus 194 (2008) 379–388
ICARUS
www.elsevier.com/locate/icarus

Radiation chemistry of $H_2O + O_2$ ices

Paul D. Cooper [a,*], Marla H. Moore [a], Reggie L. Hudson [b]

[a] *NASA/Goddard Space Flight Center, Astrochemistry Branch, Code 691, Greenbelt, MD 20771, USA*
[b] *Department of Chemistry, Eckerd College, 4200 54th Avenue South, St. Petersburg, FL 33711, USA*

Received 31 January 2007; revised 14 September 2007

Available online 26 October 2007

Abstract

The chemistry and spectroscopy of proton-irradiated $H_2O + O_2$ ices have been investigated in relation to the production of oxidants in icy satellite surfaces. Hydrogen peroxide (H_2O_2), ozone (O_3), and the hydroperoxy (HO_2) and hydrogen trioxide (HO_3) radicals have all been observed, and their temperature and dose dependent production trends have been measured. We find that O_2 aggregates form during the growth of $H_2O + O_2$ ice films, and the presence of these aggregates greatly affects the HO_2 and H_2O_2 yields. In addition, we have found that the position of the spectral maximum of the ν_3 vibration of O_3 shifts with ice composition, giving an indication of the degree of dispersion of O_3 molecules within the ice. We discuss the relevance of these measurements to icy satellite surfaces.

Keywords: Ices, IR spectroscopy; Satellites, composition; Europa; Ganymede; Enceladus

1. Introduction

Energetic radiation can alter the chemical composition of icy satellite surfaces. In the case of Europa, the destruction of water-ice is the likely source of hydrogen peroxide (H_2O_2) (Carlson et al., 1999) and molecular oxygen (O_2) (Spencer and Calvin, 2002) that have been detected there. However, O_2 formation is not unique to Europa, and mounting evidence indicates that it may occur on other icy satellites exposed to high-energy radiation. Molecular oxygen was first identified on Ganymede (Spencer et al., 1995), and has also been detected on Callisto (Spencer and Calvin, 2002). In addition, an O atom atmosphere associated with Saturn's rings suggests that O_2 is formed from the water-ice particles found there (Johnson et al., 2006). Other species that may exist in irradiated water-ice include O_3, which has been tentatively assigned to spectroscopic features of Ganymede (Noll et al., 1996; Hendrix et al., 1999), Rhea and Dione (Noll et al., 1997), the hydroxyl (OH), hydroperoxy (HO_2), and hydrogen trioxide (HO_3) radicals. The latter three species have yet to be detected in outer Solar System ices.

The spectroscopic characteristics of a molecule are often sensitive to the environment in which it is found. For example, the spectra of H_2O molecules are different in the crystalline and amorphous phases (Bergren et al., 1978; Hudson and Moore, 1992; Hudgins et al., 1993). In addition, the solid-phase spectra of many compounds are not the same in the presence and absence of water-ice (Hudgins et al., 1993; Ehrenfreund et al., 1997), mainly because of the strong hydrogen bonds present in the host water-ice matrix. These shifts are hard to predict from theory, and so experimental data are essential in characterizing them.

We recently have identified an absorption band of HO_2 in irradiated $H_2O + O_2$ ice mixtures at 1142 cm^{-1} (Cooper et al., 2006). This radical has previously been detected in irradiated ice (Bednarek et al., 1998) via electron paramagnetic resonance spectroscopy, but an infrared spectroscopic identification had until recently been elusive. In the same paper (Cooper et al., 2006), we also identified HO_3 by an absorption band at 1259 cm^{-1}. These radicals formed readily in $H_2O + O_2$ ices at 9 K and were found to also be formed at 80 K in lesser amounts. In addition, the same absorption features were observed in irradiated $H_2O + O_3$ and neat H_2O_2 ices. The latter measurement

* Corresponding author. Present address: Department of Chemistry and Biochemistry, MS 3E2, George Mason University, 4400 University Drive, Fairfax, VA 22030, USA
E-mail address: pcooper6@gmu.edu (P.D. Cooper).

0019-1035/$ – see front matter
doi:10.1016/j.icarus.2007.10.002

was recently supported by Loeffler et al. (2006a), who observed the same bands in irradiated H_2O_2 ice but did not identify them. Laffon et al. (2006) recently showed the production of H_2O_2, OH, HO_2, O_2 and O atoms simultaneously using near-edge X-ray absorption fine structure (NEXFAS) spectroscopy on H_2O ice. HO_3 and O_3 however, were not detected in their study.

Chemical species such as H_2O_2, O_2, O_3, OH, HO_2, and HO_3 are of interest to planetary scientists because they are all oxidizing agents and may provide a source of chemical energy in outer Solar System ices. Such energy has been proposed as a possibility to fuel extraterrestrial life (Chyba, 2000), although highly reactive OH and HO_2 are known to have a negative effect on living organisms. If sufficient quantities of these species exist in an ice then they may act as sterilizing agents.

Expanding on our previous work (Cooper et al., 2006), here we provide the dose and temperature dependence of HO_2 and HO_3 formation and stability in order to evaluate these radicals' potential relevance to Europa, Ganymede, and other icy outer Solar System bodies. These two radicals may also form in icy grains of the interstellar medium via cosmic ray bombardment. The formation and destruction mechanisms will be discussed, as will some other interesting observations, including a shift in the O_3 (ν_3) band position under different formation conditions.

2. Experimental methods

The experimental apparatus has been described earlier (Hudson and Moore, 1995), but in short, the ice samples were prepared by mixing the desired gas constituents in a vacuum manifold before depositing them onto a polished aluminum target held at ∼9 K by a closed-cycle helium refrigerator (APD HC-4). The pressure of the gas mixtures were measured with a capacitance manometer and were prepared such that the mixing ratios between experiments were not different by more than 2%. Water was introduced into the vacuum manifold from a bulb containing Millipore-purified H_2O, degassed using several freeze-pump-thaw cycles with liquid nitrogen. Research grade $^{16}O_2$ (Matheson Tri-Gas) or $^{18}O_2$ (Isotec; purity of >97%) was mixed with H_2O using standard manometric techniques. Ice samples were warmed at a rate of 2–3 K per minute to their irradiation temperature. The ices were then irradiated with 0.8 MeV protons from a Van de Graaff accelerator. Typical beam currents were 1×10^{-7} A over a sample area of 5.06 cm^2. Radiation doses were determined by counting the proton fluence ($p^+ cm^{-2}$) at the ice, and converting to a common scale of eV/16-amu molecule. Proton stopping powers and ranges were calculated with Ziegler's SRIM program (Ziegler et al., 1985; www.srim.org).

Sample thickness was measured by counting laser interference fringes and was typically 3 μm, deposited at a rate of ∼0.1 μm min^{-1}. Three-micron thick samples were found to be ideal as they provided the best signal-to-noise ratio for the small HO_2 and HO_3 absorptions, without too much baseline distortion from the strongly absorbing water bands. A gas-phase $H_2O + O_2$ ratio of 6:1 was chosen for many experiments, as a compromise between 1:1, which gave poor quality spectral characteristics, and 10:1, which gave low HO_2, HO_3, and O_3 absorbances.

Infrared (IR) spectra were obtained using a Nexus 670 spectrometer with 100 scans at 4 cm^{-1} resolution. In these experiments the IR bream was transmitted through the ice, reflected from the metal mirror substrate, and was re-transmitted through the ice before entering the detector. Each sample spectrum was divided by the reflectance spectrum from the blank aluminum substrate. These ratioed spectra were converted to $-\log(I/I_O)$ (absorbance), and band areas of interest (H_2O_2, O_3, HO_2, and HO_3) were calculated using an appropriate baseline.

3. Results

3.1. Irradiation of $H_2O + O_2$ ices

Fig. 1 shows the mid-IR spectral changes of a 6:1 $H_2O + O_2$ ice mixture irradiated to a dose of 0.6 eV/16 amu at 9 K. Before irradiation, the forbidden 1550 cm^{-1} O_2 vibrational band was also observed along with a small CO_2 impurity at 2344 cm^{-1}. After irradiation new features at 2850, 1259, 1142, and 1039 cm^{-1} appear in the spectrum. A decrease in intensity of the small absorption band at ∼3673 cm^{-1}, associated with dangling OH bonds (Rowland et al., 1991), was observed and was consistent with previous work (Palumbo, 2006). The 2850 and 1039 cm^{-1} absorptions produced by H_2O_2 and O_3, respectively, have been well characterized in the literature (Moore and Hudson, 2000; Loeffler et al., 2006a). The 1259 and 1142 cm^{-1} features were recently shown in this laboratory to be from HO_3 and HO_2 radicals (Cooper et al., 2006), respectively.

3.2. Spectral positions of ozone

Fig. 2 shows the ν_3 band of O_3 synthesized in different ices. Spectrum (a) is the absorption of O_3 produced in a 1:1 H_2O +

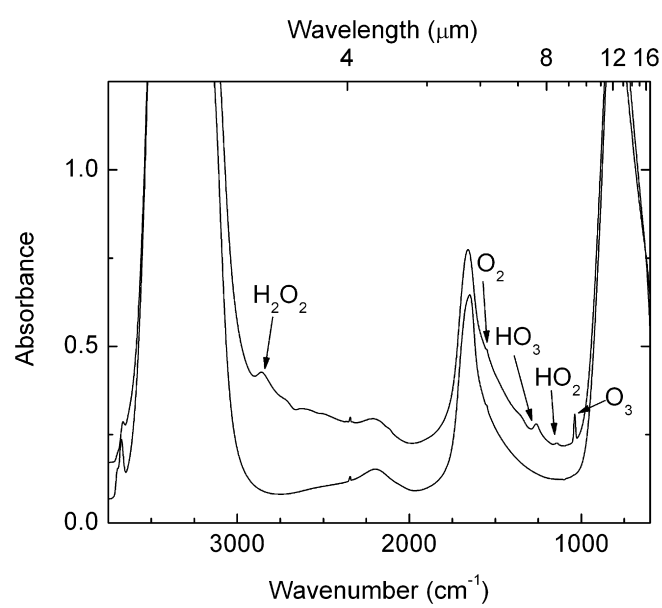

Fig. 1. Spectral changes in a 6:1 $H_2O + O_2$ ice at 9 K after a radiation dose of 0.6 eV/16 amu.

O_2 irradiated mixture at 10 K while (b) is from a 6:1 $H_2O + O_2$ sample at the same temperature. Warming the latter ice mixture to 50 K produced (c) and further warming to 125 K gave (d).

3.3. H_2O_2 formation vs temperature

Fig. 3 shows the change in area of the ~2850 cm^{-1} H_2O_2 absorption band with increasing radiation dose for 6:1 $H_2O + O_2$ ices at temperatures between 9 and 100 K. The band appears as a shoulder on the much larger water absorption at ~3300 cm^{-1}. The H_2O_2 band area was calculated by subtracting the spectrum of a pre-irradiated ice mixture from the spectrum of a post-irradiated ice mixture. The band area was then measured from this difference spectrum.

H_2O_2 is formed slowly at first and then begins to rapidly increase with higher dose, before reaching a steady-state value at ~5 eV/16 amu. The value of the H_2O_2 area at steady-state decreases between 9 and 35 K and is probably associated with the loss of O_2 from the sample at ~30 K. The area then does not change much between 35 and 50 K but rises at 80 K, before decreasing once again at 100 K.

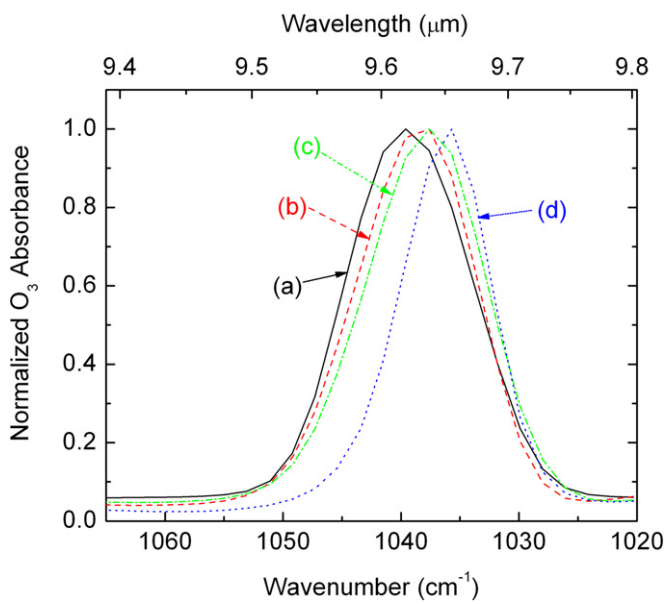

Fig. 2. The ν_3 band of O_3 formed in an (a) irradiated 1:1 $H_2O + O_2$ ice at 10 K; (b) irradiated 6:1 $H_2O + O_2$ ice at 9 K; (c, b) warmed to 50 K; (d, b) warmed to 125 K.

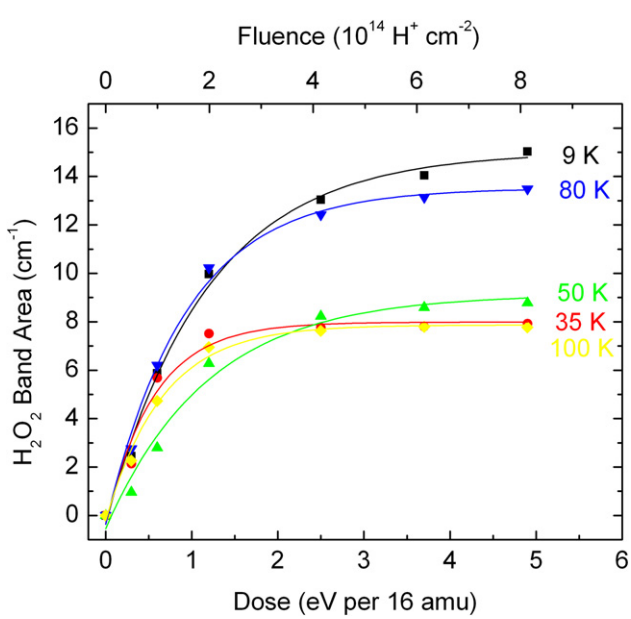

Fig. 3. The dose dependent formation of H_2O_2 in a 6:1 $H_2O + O_2$ ice at 9, 35, 50, 80, and 100 K.

3.4. O_3 formation vs temperature

Fig. 4 shows the change in the 1039 cm^{-1} O_3 band area as a function of dose and temperature. The saturated peak intensity decreases with increasing irradiation temperature. The large drop in band area between 9 and 35 K is due to the sublimation of some of the O_2 at ~30 K. Loeffler et al. (2006b) report that ~3% O_2 and O_3 is lost between 35 and 90 K in similar experiments. This is too small to account for the ~50% decrease in O_3 absorbance between 35 and 80 K in the present experiments. However, Chaabouni et al. (2000) report a steady decrease in O_3 desorption between 60 and 100 K in their non-irradiation experiments and attributed it to a physisorbed state of O_3 that is identical in spectral properties to pure O_3. Other possibilities to explain the lower yield of O_3 include a temperature dependent formation mechanism or an increased destruction rate at higher temperature.

3.5. HO_2 formation vs temperature

Fig. 5 shows the integrated absorbance of the HO_2 band as a function of dose at temperatures between 9 and 100 K. The band area of the HO_2 feature decreased with increasing temperature except for the initial change in temperature between 9 and

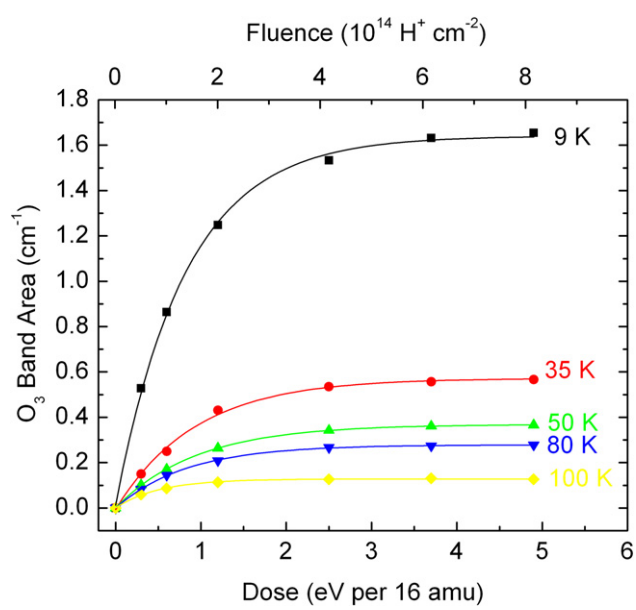

Fig. 4. The dose dependent formation of O_3 in a 6:1 $H_2O + O_2$ ice at 9, 35, 50, 80, and 100 K.

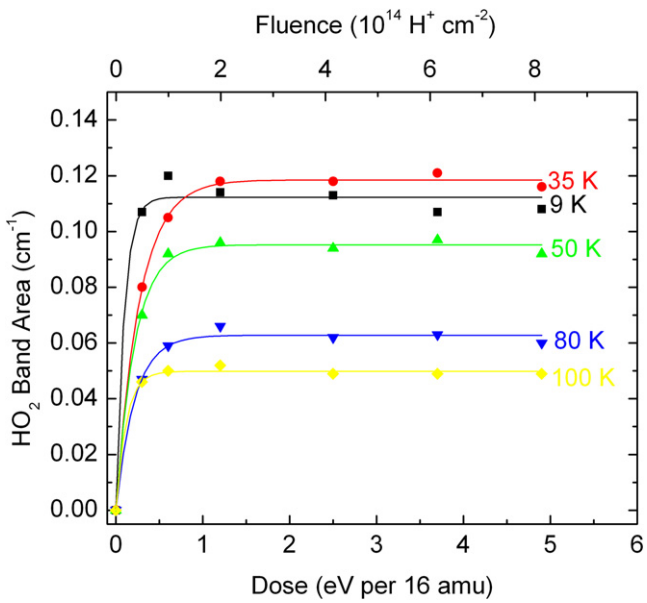

Fig. 5. The dose dependent formation of HO_2 in a 6:1 $H_2O + O_2$ ice at 9, 35, 50, 80, and 100 K.

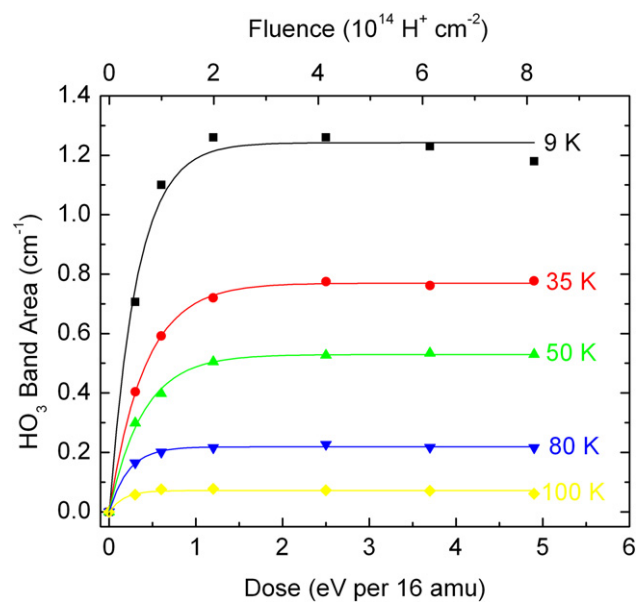

Fig. 6. The dose dependent formation of HO_3 in a 6:1 $H_2O + O_2$ ice at 9, 35, 50, 80, and 100 K.

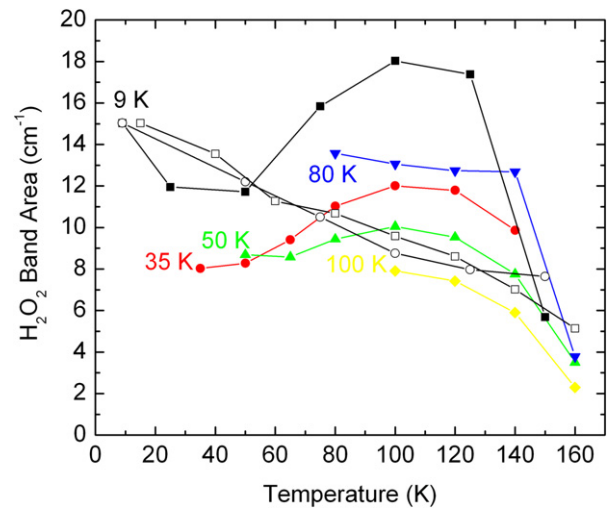

Fig. 7. The change in H_2O_2 band area upon warming 6:1 $H_2O + O_2$ ices irradiated to steady-state conditions (∼5 eV/16 amu) at 9, 35, 50, 80, and 100 K. The unfilled square and circular data points show the intensity change of the ∼2850 cm^{-1} band upon warming unirradiated H_2O_2 and a 3% H_2O_2 in H_2O ice sample, these data were scaled to the 9 K $H_2O + O_2$ irradiated data in order to provide a comparison.

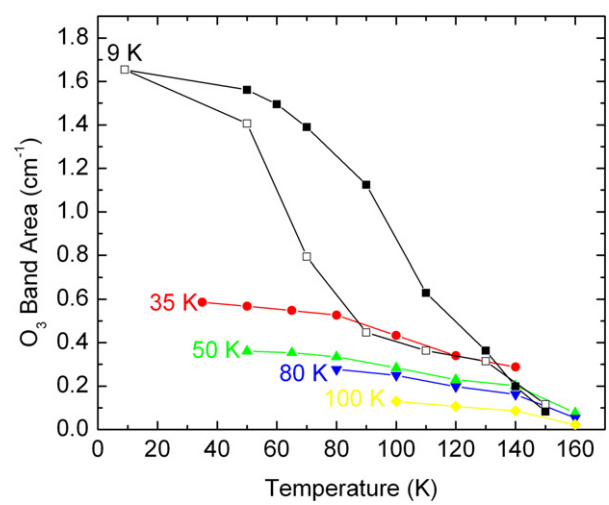

Fig. 8. The change in O_3 band area upon warming 6:1 $H_2O + O_2$ ices irradiated to steady-state conditions (∼5 eV/16 amu) at 9, 35, 50, 80, and 100 K. The unfilled square data points show the O_3 loss from an unirradiated ∼5:1 $H_2O + O_3$ mixture, co-deposited at 9 K and warmed to 150 K. The data of the co-deposited mixture was scaled to the 9 K $H_2O + O_2$ irradiated data in order to provide a comparison.

35 K. The amount of HO_2 produced was about the same at 9 and 35 K but was formed slightly slower at 35 K than at 9 K.

3.6. HO_3 formation vs temperature

Fig. 6 shows that HO_3 was formed rapidly with increasing radiation dose. The radical's steady-state IR band area decreases with increasing temperature. We previously showed (Cooper et al., 2006) that HO_3 forms via H addition to O_3, and so a decrease in O_3 (Fig. 4) reduces the amount of HO_3 produced and probably accounts for much of the fall in HO_3 intensity. The HO_3 decrease between 9 and 35 K was not as great as it was for O_3. The reason for this will be discussed in the next section.

3.7. Stability of radiation products vs temperature

Figs. 7 and 8 show the effect of warming an $H_2O + O_2$ ice irradiated at 9, 35, 50, 80 and 100 K on the area of the H_2O_2 and O_3 bands, respectively. H_2O_2 displays a complex behavior during warming while O_3 decreases with increasing temperature. The band area of H_2O_2 in ices irradiated at 9, 35, and 50 K increases to a maximum between 80 and 120 K before decreasing again. In 80 and 100 K irradiated samples, the H_2O_2 band

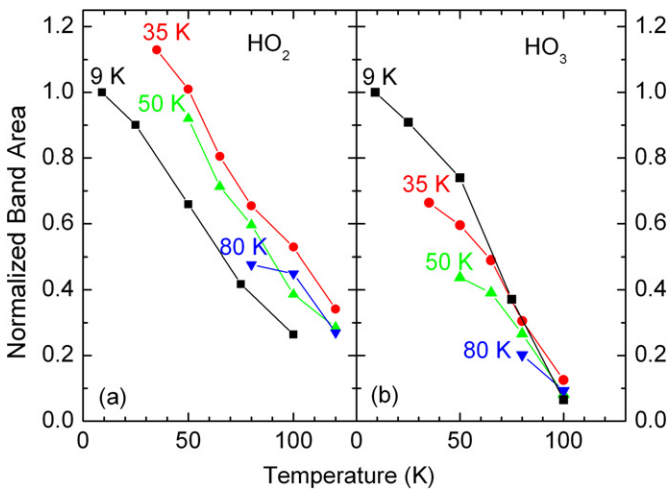

Fig. 9. The change in (a) HO_2 and (b) HO_3 normalized band area upon warming 6:1 $H_2O + O_2$ ices irradiated to steady-state conditions (∼5 eV/16 amu) at 9, 35, 50, and 80 K.

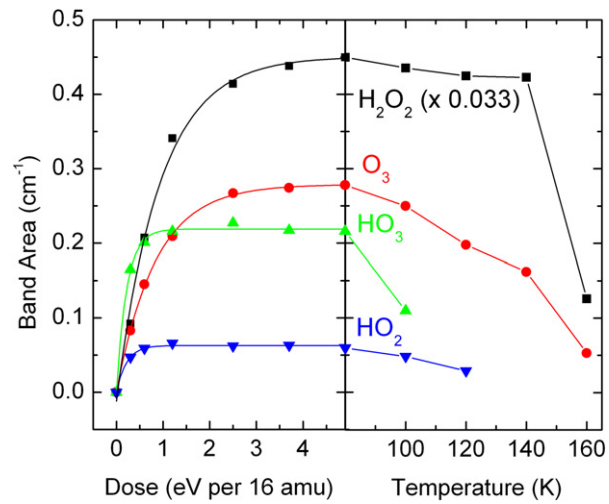

Fig. 10. A comparison of the formation of H_2O_2, O_3, HO_2, and HO_3 at 80 K and subsequent removal (via either destruction or desorption) from the ice as it is warmed from 80 to 160 K.

area stays about the same before decreasing above 120 K. For comparison, Fig. 7 also shows the effect of temperature on non-irradiated pure H_2O_2 and 3% H_2O_2 in H_2O ice samples. The observed band area of H_2O_2 in each of these samples actually decreases monotonically with increasing temperature. Loeffler et al. (2006b) found that H_2O_2 sublimation was negligible at the temperatures used in the present experiments. Therefore the montonic decrease could be due to a decrease in the intrinsic band strength with increasing temperature or is only apparently decreasing due to changes in the optical properties of the sample. Nevertheless, we observe an increase in the band area of H_2O_2 in irradiated $H_2O + O_2$ ices as the temperature is increased up to 120 K.

The band area of O_3 plotted in Fig. 8 decreases monotonically with increasing temperature. For comparison, Fig. 8 also shows the effect of warming an unirradiated 5:1 $H_2O + O_3$ mixture co-deposited at 9 K. The O_3 in this unirradiated sample was less thermally stable than O_3 formed radiolytically in irradiated $H_2O + O_2$ mixtures.

Fig. 9 shows the effect of warming an irradiated $H_2O + O_2$ ice on the amount of HO_2 and HO_3. For comparison, the integrated bands have been normalized to the area for that species at 9 K. Both radicals are destroyed as the temperature increases, however HO_2 destruction was slightly slower and persists to a slightly higher temperature.

Fig. 10 compares the formation and destruction data at 80 K for all four species of interest. The H_2O_2 band areas have been reduced by a factor of 25 in order to display the peroxide on the same graph with O_3, HO_2, and HO_3.

4. Discussion

4.1. O_2 and O_3

In the present experiments, different H_2O:O_2 ratios were used, to elucidate the variety of O_2 bonding environments in the ice. Some O_2 molecules will have only H_2O molecules as nearest neighbors, while some will be surrounded by a mixture of O_2 and H_2O. At the latter locations, O_2 may actually be present in small aggregates within the ice and will consequently behave like bulk solid oxygen. It is these aggregates that sublime when the sample is warmed to 30 K or higher. Acting as a tracer molecule, the O_3 band position may provide information about the state of O_2 in the ice since the spectral maximum of the ν_3 mode of O_3 is shifted when bonded to water (Schriver et al., 1990). Under different conditions, the O_3 in our ice samples may form in O_2 aggregates or be dispersed within the ice lattice.

Pure amorphous and crystalline-phase O_3 produce their strongest band, ν_3, at 1037.1 and 1026.9 cm^{-1}, respectively (Chaabouni et al., 2000), while O_3 in an O_2 matrix produces a band at 1037.8 cm^{-1} (Schriver-Mazzuoli et al., 1995) and in an N_2 matrix at 1043.0 cm^{-1} (Schriver-Mazzuoli et al., 1996). An O_3 dimer in an O_2 matrix produces a feature at 1042 cm^{-1} (Bennett and Kaiser, 2005). Table 1 summarizes band positions for O_3 in various ices. Fig. 2a shows the absorption of O_3 with a spectral maximum at 1039.7 cm^{-1} from an irradiated 1:1 $H_2O + O_2$ ice mixture at 9 K. At this ratio, O_3 monomers and dimers will be mostly formed in oxygen-rich environments due to the large abundance of O_2. The absorptions at 1038 and 1042 cm^{-1} cannot be resolved at our spectral resolution of 4 cm^{-1}, but a contribution from both is likely. Our observed spectral maximum at 1039.7 cm^{-1} lies between the maxima for O_3 monomer and dimer, and is consistent with a mixture of both being present.

Spectrum (b) in Fig. 2 shows the ozone absorption in an irradiated 6:1 $H_2O + O_2$ ice at 9 K. The lower fraction of O_2 should produce fewer O_3 dimers, and this is supported by the small shift to lower frequency of the spectral maximum to 1038.5 cm^{-1}. The O_3 dimer absorption on the high energy side of the band is reduced, resulting in a shift of the peak. When the sample is warmed to 50 K, the maximum shifts to 1037.8 cm^{-1} (c), and then again to 1035.8 cm^{-1} (d) at 125 K. These changes can be interpreted as the gradual loss of O_3 monomer from an

Table 1
Summary of spectral maxima (cm^{-1}) for the $\nu_3(O_3)$ absorption band

O_3 in various ices	Temperature (K)	ν_3 band position (cm^{-1})	Reference
Pure amorphous O_3	11	1037.1	Chaabouni et al. (2000)
Pure crystalline O_3	55	1026.9	Chaabouni et al. (2000)
O_3 in an N_2 matrix	11	1043.0	Schriver-Mazzuoli et al. (1996)
O_3 in an O_2 matrix	11	1037.8	Schriver-Mazzuoli et al. (1995)
O_3 dimer in an O_2 matrix	11	1042	Bennett and Kaiser (2005)
O_3 H-bonded to H_2O	11	1033.8	Schriver et al. (1990)
O_3 formed in irradiated $H_2O + O_2$ ices			
O_3 in $H_2O + O_2$ (1:1)	9	1039.7	This work
O_3 in $H_2O + O_2$ (6:1)	9	1038.5	This work
O_3 in $H_2O + O_2$ (10:1)	9	1036.2	This work
O_3 in $H_2O + O_2$ (6:1)	9	1038.5	This work
O_3 in $H_2O + O_2$ (6:1)	50	1037.8	This work
O_3 in $H_2O + O_2$ (6:1)	125	1035.8	This work

Table 2
Parameters[a] for the pseudo-first order formation of H_2O_2, O_3, HO_2, and HO_3

		9 K	35 K	50 K	80 K	100 K
H_2O_2	b	15.3 ± 0.5	8.3 ± 0.7	9.7 ± 0.6	13.9 ± 0.5	8.0 ± 0.4
	k	0.85 ± 0.08	1.8 ± 0.3	0.85 ± 0.16	1.1 ± 0.1	1.5 ± 0.2
O_3	b	1.6 ± 0.01	0.77 ± 0.01	0.36 ± 0.01	0.28 ± 0.01	0.13 ± 0.01
	k	1.2 ± 0.1	1.1 ± 0.1	1.1 ± 0.1	1.2 ± 0.1	2.0 ± 0.2
HO_2	b	0.11 ± 0.01	0.12 ± 0.01	0.10 ± 0.01	0.06 ± 0.01	0.05 ± 0.01
	k	10.6 ± 3.6	3.7 ± 0.2	4.6 ± 0.3	4.7 ± 0.5	8.6 ± 0.9
HO_3	b	1.3 ± 0.03	0.77 ± 0.01	0.53 ± 0.01	0.22 ± 0.01	0.07 ± 0.01
	k	3.2 ± 0.3	2.5 ± 0.05	2.6 ± 0.1	4.6 ± 0.7	6.3 ± 2.2

[a] Data were fitted to the equation $A(D) = b(1 - e^{-kD})$, where D is the dose in eV/16 amu and A is band area with units of cm^{-1}. b and k are constants that characterize each curve.

O_2-rich environment, and the gradual increase of O_3 monomer that is hydrogen bonded to the water molecules in the ice. The latter is known to absorb at 1033.8 cm^{-1} (Schriver et al., 1990). A 10:1 $H_2O + O_2$ ice was also irradiated at 9 K and the O_3 band position was observed at 1036.2 cm^{-1} (not shown), entirely in agreement with our reasoning above.

Table 1 also summarizes the positions of the ν_3 band of O_3 for $H_2O + O_2$ ices irradiated at different temperatures. From these data we can see that the O_2 sublimation at ∼30 K has a large effect on the spectral position of O_3. The O_2 subliming from the sample comes from aggregates behaving like bulk solid O_2, while the O_2 molecules remaining trapped are more dispersed in the water-ice, producing a greater fraction of hydrogen-bonded O_3 molecules. This is consistent with the shift of the band maximum to a lower frequency (see Table 1). The amount of O_3 also significantly decreases with increasing irradiation temperature as shown in Fig. 4. It is much easier to form O_3 in an aggregate of O_2 molecules than from O_2 molecules dispersed throughout the ice lattice. The data in Fig. 4 are fitted by a first-order curve and the parameters are listed in Table 2. These fits are consistent with a pseudo-first-order reaction mechanism in which O_2 is in excess (Eq. (1)).

$$O_2 + O \rightarrow O_3. \quad (1)$$

For a comprehensive investigation of the formation mechanism of O_3 in the solid-state, see the work by Baragiola et al. (1999). Ozone is made from an O_2 molecule (with the addition of another O atom), and so the degree of dispersion of O_3 molecules is an indirect measurement of the degree of dispersion of O_2 molecules. This is important for studies of Ganymede and Europa where the O_2 is thought to be present in high densities (Calvin et al., 1996) and possibly aggregates where O_2/O_3 'microatmospheres' may exist (Johnson and Jesser, 1997).

4.2. HO_2 and HO_3

Further evidence for the presence of O_2 aggregates at 9 K comes from the band positions of HO_2 and HO_3 observed in $H_2O + O_2$ ices irradiated at different temperatures (Table 3). A shift in the HO_2 band position occurs above the sublimation point of O_2 (∼30 K), indicating that HO_2 is formed in a different location within the ice above this temperature. The lowering of the frequency with increasing irradiation temperature is consistent with an increase in hydrogen bonding of the HO_2 radical (Nelander, 1997). HO_3 also shifts with increasing irradiation temperature and again the direction of the shift indicates the effect of increased hydrogen bonding. The higher temperatures may also allow radicals to gain sufficient thermal energy to reposition themselves into lower-energy configurations within the

Table 3
Spectral positions for $\tilde{\nu}_3$ ($H^{16}O_2$) and $\tilde{\nu}$ ($H^{16}O_3$) bands formed at different temperatures

	$\tilde{\nu}_3$ ($H^{16}O_2$) (cm^{-1})	$\tilde{\nu}_3$ ($H^{18}O_2$) (cm^{-1})	Isotopic shift (cm^{-1})	$\tilde{\nu}_3$ ($H^{16}O_2$)/$\tilde{\nu}_3$ ($H^{18}O_2$)
In H_2O-ice 9 K	1142	1078	64	1.059
In H_2O-ice 35 K	1135	–	–	–
In H_2O-ice 50 K	1135	–	–	–
In H_2O-ice 80 K	1135	1072	63	1.059
In H_2O-ice 100 K	1135	–	–	–
In Ar	1101.3	1039.7	61.6	1.0592
	$\tilde{\nu}_3$ ($H^{16}O_3$) (cm^{-1})	$\tilde{\nu}_3$ ($H^{18}O_3$) (cm^{-1})	Isotopic shift (cm^{-1})	$\tilde{\nu}_3$ ($H^{16}O_3$)/$\tilde{\nu}_3$ ($H^{18}O_3$)
In H_2O-ice 9 K	1259	1220	39	1.032
In H_2O-ice 35 K	1259	–	–	–
In H_2O-ice 50 K	1258	–	–	–
In H_2O-ice 80 K	1256	1221	35	1.029
In H_2O-ice 100 K	1254	–	–	–
In Ar	1223	1190	33	1.028

Positions for the 18-oxygen substituted isotopomers are shown at 9 and 80 K.

lattice. We noted in our previous paper (Cooper et al., 2006) that the isotopic shift for HO_3 in H_2O at 9 K was higher than the shift in Ar (Table 3). Earlier work (Nelander et al., 2000) showed that the HO_3 vibration we followed has both bending and stretching components, and so we proposed (Cooper et al., 2006) that the ice matrix slightly affects the relative contribution of each vibrational component, due to the geometrical constraints of accommodating the large HO_3 species into the H_2O lattice. This alteration appears to indeed be the case, because the agreement in the isotopic shift at 80 K and the shift in Ar is much better than at 9 K (Table 3).

If we now turn to the dependence of HO_3 formation on irradiation temperature, Fig. 6 shows that the saturation amount of HO_3 decreases with increasing temperature. This trend is expected from the decrease in the amount of O_3 produced, as just discussed. However, the O_3 decrease between 9 and 35 K is far greater (∼62%) than that of HO_3 (∼38%) over the same temperature range. The likely reason for this is that at 9 K the O_3 is produced in O_2 clusters, as already discussed. In such an environment, an HO_3 will have a short lifetime because of reactions with other HO_3 and HO_2 radicals made concurrently within the aggregate. Since little is known about HO_3 chemistry, we cannot say whether or not this radical will react with O_2 or O_3 molecules. Overall, reactions of HO_3 will limit this radical's concentration in the clusters in which it is formed, and this results in less HO_3 being produced than might be expected from the amount of O_3 present. HO_3 formed from dispersed O_3 molecules at temperatures greater than 30 K is stabilized by hydrogen bonding (Aloisio and Francisco, 1999) and is the likely source of most of the HO_3 in the ice.

Similarly, the HO_2 band area decreases with increasing temperature except for the 9–35 K interval (Fig. 5). The amounts of HO_2 at 9 and 35 K are roughly the same, although at 35 K it takes a higher radiation dose to reach a steady-state level. Once again, the likely reason why the band area at 9 K is lower than expected from the trend is because of formation and subsequent self-reaction within an O_2 aggregate. Supporting this assertion is the higher than expected amount of H_2O_2 at 9 K in Fig. 3. The trend between 35 and 80 K is for the H_2O_2 to increase, but the 9 K data is higher than expected from this trend. The reason for this is likely to be that H_2O_2 is produced from the disproportionation of HO_2 in O_2 clusters.

$$HO_2 + HO_2 \rightarrow H_2O_2 + O_2. \quad (2)$$

So at 9 K, the HO_2 concentration is limited by the fact that many HO_2 radicals are formed in close proximity in O_2 aggregates through the combination of O_2 and H atoms produced from the dissociation of H_2O.

The reason for the decrease in HO_2 yield above 35 K may be similar to that of HO_3. The amount of O_2 remaining in the ice as the temperature is raised will decrease due to thermal desorption. However, this loss cannot be measured via IR spectroscopy because of the extremely weak O_2 IR band. Chemical reactions that occur as the mobility of reactive species increases with higher temperatures may also contribute to the loss of HO_2 above 35 K.

In our earlier paper (Cooper et al., 2006), we discussed possible formation paths for HO_2 and HO_3. The expanded data here allows us to draw the conclusion that H-addition reactions to O_2 and O_3 are the dominant mechanisms. First-order fits in Figs. 5 and 6 are consistent with pseudo-first-order reactions where O_2 and O_3 are in excess. See Table 2 for a list of the parameters of the curves fitted to the data in Figs. 5 and 6. These first-order fits are made by assuming that the abundances of radiolytic fragments (such as H, OH, and O) are small compared with those of H_2O, O_2, and O_3.

4.3. H_2O_2

It would appear that H_2O_2 can be formed by a number of different mechanisms in the present set of experiments. Three possibilities are H-atom addition (Eqs. (3a) and (3b)), HO_2 disproportionation (Eq. (2)), and OH dimerization (Eq. (4)). It was previously suggested that two H-addition reactions to O_2 (to form HO_2 as an intermediate) enhanced the production of H_2O_2 in irradiated $H_2O + O_2$ ices (Moore and Hudson, 2000; Cooper et al., 2006).

$$H + O_2 \rightarrow HO_2, \quad (3a)$$

$$H + HO_2 \rightarrow H_2O_2. \quad (3b)$$

However, at 9 K it is possible that the first step in this sequence (Eq. (3a)) occurs only in O_2 aggregates, so that before a second H can react with HO_2 (Eq. (3b)), two neighboring HO_2 radicals combine with one another, to give H_2O_2 and O_2 (Eq. (2)). This explains the greater yield of H_2O_2 at 9 K compared with 35 K. Above 35 K there are fewer O_2 aggregates in the ice, and so HO_2 is formed and remains trapped before reacting with a second H to produce H_2O_2.

At 80 K an increase in the H_2O_2 band area was measured. The most commonly proposed H_2O_2 formation mechanism, is that of the reaction of two OH radicals.

$$OH + OH \rightarrow H_2O_2. \tag{4}$$

These OH radicals are strongly hydrogen bonded to water molecules (Cooper et al., 2003), and it is not until ∼80 K that they can diffuse within a water-ice lattice (Johnson and Quickenden, 1997, and references therein). Energetic OH radicals can diffuse short distances along ion tracks and react at 10 K, but bulk diffusion probably does not occur. The increase of H_2O_2 at 80 K we observe is probably an effect of this OH mobility. At 100 K the H_2O_2 abundance decreases dramatically and reflects increased destruction of H_2O_2 by reactive species such as OH radicals or electrons.

Without the presence of O_2, a detectable quantity of H_2O_2 is not seen at 80 K in our proton-irradiated H_2O. This result is consistent with Moore and Hudson (2000). They suggested that one possible reason why H_2O_2 was not observed in proton MeV irradiation experiments on pure H_2O at 80 K was because of the rapid reaction of electrons with H_2O_2. When electron-scavenging molecules were co-deposited with water, H_2O_2 was produced in observable quantities. Molecular oxygen may also be acting as an electron scavenger in the present experiments via the formation of the superoxide ion (O_2^-). The role of electron scavenging needs to be investigated further but is beyond the scope of the present paper. Other groups (Loeffler et al., 2006c; Gomis et al., 2004a, 2004b) recently have shown that observable amounts of H_2O_2 can be produced in pure H_2O at 80 K using keV-energy ions with greater stopping power than 0.8 MeV protons. Researchers Zheng et al. (2006b) and Loeffler et al. (2006c) reported a decrease in H_2O_2 production in pure water-ice with increasing temperature, and so electron scavenging may play a critical role in the radiation stability of H_2O_2 in the ice in our experiments. However, Gomis et al. (2004a) found that the yields were ion-dependent. Ices irradiated with C^+, H^+ and O^+ ions produced more H_2O_2 at 77 K than 16 K, while N^+ and Ar^+ had no temperature dependence on the H_2O_2 yield.

Yet a fourth reaction sequence, discussed by Zheng et al. (2006a), is O addition to H_2O to form H_2O_2. Although there is no clear evidence from our data for it, O atoms produced from the dissociation of O_2 may react with H_2O to form H_2O_2.

4.4. Chemical destruction processes

Once the ice at each temperature was irradiated and the formation of products approached steady-state values, the sample was warmed. Figs. 7–9 show the changes in the band areas of H_2O_2, O_3, HO_2, and HO_3. The loss of O_3 (Fig. 8) may be due to desorption from the ice, but the increased rate of loss between 80 and 120 K may also indicate a chemical destruction mechanism. Fig. 9 shows that HO_2 and HO_3 are destroyed at ∼100–120 K. The diffusion of these species in ice is not well understood. The OH radical, which is comparable to HO_2 in terms of the strength of hydrogen bonding (Cooper et al., 2003; Nelander, 1997), is mobile at these temperatures, but the larger physical sizes of HO_2 and HO_3 may significantly affect their mobility.

The increase in H_2O_2 (Fig. 7) after warming irradiated 9, 35 and 50 K $H_2O + O_2$ ices is likely the result of trapped OH radicals reacting with one another, as in Eq. (4). OH radicals are produced at all temperatures. An OH radical that can reactively scatter to within close proximity of another OH can combine with it to form H_2O_2, but at the lower temperatures if an OH does not react then it will be trapped in the ice lattice. As the ice's temperature increases, the OH mobility rises and more H_2O_2 is produced. However, OH also destroys H_2O_2 as follows:

$$OH + H_2O_2 \rightarrow HO_2 + H_2O. \tag{5}$$

In other words, the H_2O_2 concentration is enhanced, but also limited by the availability of OH radicals. In experiments on 80 and 100 K irradiated samples, no increase in H_2O_2 is seen during warming, indicating that the rate of H_2O_2 formation is about equal to the rate of destruction of H_2O_2 by Eq. (5). Alternatively there may not be enough OH radicals stored during irradiation at 80 K or 100 K to bring about an increase in the H_2O_2 concentration with further warming. For all cases investigated here, the H_2O_2 concentration starts to decrease once the irradiated ice temperature exceeds 120 K. The decrease between 120 and 160 K is not attributed to thermal losses since Zheng et al. (2006a) showed that warmed H_2O-ice containing H_2O_2 did not release H_2O_2 until the 160–180 K region. The decrease we observe therefore suggests that OH radicals are rapidly destroying H_2O_2. The product of this destruction, HO_2 is not seen to increase as would be expected, because it too is rapidly destroyed by OH (Eq. (6)).

$$OH + HO_2 \rightarrow H_2O + O_2. \tag{6}$$

However, destruction of HO_2 is slower than that of HO_3, so that HO_2 remains in the ice to a temperature ∼20 K higher than HO_3. A reservoir of H_2O_2 would buffer the HO_2 concentration and explains this observation. The chemistry of H_2O_2, O_3, HO_2 and HO_3 with OH radicals is supported by recent work by Loeffler et al. (2006b) who observed a decrease in O_3 concentration in irradiated H_2O_2 associated with a chemical destruction mechanism. The reaction of OH with O_3 may also produce HO_2 via Eq. (7) and could also contribute to HO_2 persisting in the ice at a higher temperature than HO_3.

$$OH + O_3 \rightarrow HO_2 + O_2. \tag{7}$$

4.5. Relevance to icy satellites

We have shown that irradiated $H_2O + O_2$ ices produce H_2O_2, O_3, HO_2, and HO_3. All of these new species are ox-

idizing agents and may provide chemical energy to the surfaces and potentially to any liquid sub-surfaces that may exist on the icy Galilean satellites. We have formed H_2O_2 at much higher amounts in the presence of O_2 in the ice than without, which raises the question of how H_2O_2 is formed on such icy satellites and what is its relation to the chemistry of O_2?

The products of liquid water's radiolysis usually are discussed in terms of chemical reactions that first produce OH, then H_2O_2, then HO_2, and finally O_2. In contrast, the radiolysis of water-ice, which is more relevant to planetary scientists, has proven more difficult to interpret. If the combination of two OH radicals (Eq. (4)) produced from the radiolytic destruction of water-ice forms H_2O_2, then this molecule could be destroyed by radiation to form O_2 (Loeffler et al., 2006a). Alternatively, if O_2 is produced first (Johnson et al., 2005; Petrik et al., 2006), then subsequent H-addition reactions (Eqs. (3a) and (3b)) could produce H_2O_2. Recent work (Petrik et al., 2006) has suggested that in 87 eV electron irradiation of water-ice, H_2O_2 forms first via Eq. (4), before Eq. (5) produces HO_2. The latter then undergoes an electronic excitation to give O_2. However, Petrik et al. (2006) also proposed that HO_2 is a stable precursor for O_2 at temperatures as high as 130 K. In fact, the O_2 yield in their experiments, as in earlier studies (Johnson et al., 2005; Orlando and Sieger, 2003), increased with temperature. We do not see HO_2 being stable above 100 K, as the amount of HO_2 present after saturation doses (>1 eV/16 amu) decreases with increasing temperature. The greater penetrating range of MeV protons and much higher dose used in the present work compared with that of Petrik et al. (2006) may contribute to this difference. Further comprehensive and systematic investigations of O_2 formation are needed to sort out the influence of different temperature and radiation environments.

As an alternative to the above, H_2O_2 and O_2 may form independently of one another directly from H_2O and then subsequently interconvert. Further work needs to be carried out to determine this. What is clear though is that H_2O_2 and O_2 are likely to be present together on icy satellite surfaces because of their intimately related radiation chemistry in water-ice.

In addition, O_3 may also be spatially correlated with H_2O_2 and O_2 on icy satellites since O_3 is formed easily in O_2 clusters. If O_3 forms in O_2-rich regions, then the ν_3 band maximum will be at $\sim$1038–1040 cm^{-1}, but if the peak is at 1035–1036 cm^{-1}, then this would indicate that the O_3 is dispersed in the water-ice. The O_3 molecule would in effect be acting as a tracer for O_2 and would provide an indication of its state.

HO_2 and HO_3 radicals may also be present on the Galilean satellites, and might be expected to be found in greater column densities at the colder polar regions. The band areas of these species decrease with increasing temperature and by $\sim$100 K, we were unable to detect their infrared bands in our laboratory samples. Interestingly, the $HO_2{\cdot}H_2O$ complex is calculated (Aloisio et al., 1999) to have a UV absorption at 255 nm, compared with 192 nm for the free HO_2 radical. HO_2 in water-ice may contribute to the 'ozone-like absorber' band observed near 260 nm by the Galileo ultraviolet spectrometer (UVS) instrument (Hendrix et al., 1999).

5. Conclusions

The major conclusions from this work are summarized below.

1) The position of the ν_3 band of O_3 is sensitive to the environment in which the molecule is situated. When an O_3 is surrounded by O_2 molecules the spectral maximum occurs at 1038.5 cm^{-1}. The peak shifts to 1035.6 cm^{-1} when O_3 is surrounded by water molecules.
2) HO_2 and HO_3 are produced in O_2-containing ices and are present at a detectable level up to $\sim$100 K.
3) The H_2O_2 growth observed on warming irradiated $H_2O + O_2$ ices suggests that some OH radicals produced below 80 K are trapped and do not react until the 80–120 K temperature range.
4) For O_3, HO_2, and HO_3, the trend upon warming of the irradiated $H_2O + O_2$ ices is for these species to decrease in abundance. Some O_3 is lost via desorption from the ice, however a loss via chemical destruction appears to occur. Mobile OH radicals are the most likely source for the destruction of these species.
5) A variety of oxidizing species, including H_2O_2, O_3, OH, HO_2, and HO_3 are all produced in $H_2O + O_2$ ices and likely part of the oxidant inventory on icy satellites such as Europa and Enceladus. These species may provide chemical energy to sub-surface water that may potentially harbor non-Earth originating life.

Acknowledgments

The authors acknowledge support through The Goddard Center for Astrobiology, and NASA's Laboratory for Planetary Atmospheres and Planetary Geology and Geophysics programs. In addition, we thank Steve Brown, Claude Smith, and Eugene Gerashchenko, members of the Radiation Laboratory at NASA Goddard, for operation of the accelerator. R.L.H. acknowledges support from NASA Grant NNG05-GJ46G. P.D.C. acknowledges support from a NASA Postdoctoral Fellowship.

References

Aloisio, S., Francisco, J.S., 1999. Water complexation as a means of stabilizing the metastable HO_3 radical. J. Am. Chem. Soc. 121, 8592–8596.

Aloisio, S., Li, Y., Francisco, J.S., 1999. Complete active space self-consistent field and multireference configuration interaction studies of the differences between the low-lying excited states of HO_2 and HO_2–H_2O. J. Chem. Phys. 110, 9017–9019.

Baragiola, R.A., Atterbury, C.L., Bahr, D.A., Jakas, M.M., 1999. Solid-state ozone synthesis by energetic ions. Nucl. Instr. Meth. B 157, 233–238.

Bednarek, J., Plonka, A., Hallbrucker, A., Mayer, E., 1998. Radical generation upon gamma-irradiation of two amorphous and two crystalline forms of water at 77. J. Phys. Chem. A 102, 9091–9094.

Bennett, C.J., Kaiser, R.I., 2005. Laboratory studies on the formation of ozone (O_3) on icy satellites and on interstellar and cometary ices. Astrophys. J. 635, 1362–1369.

Bergren, M.S., Schuh, D., Sceats, M.G., Rice, S.A., 1978. The OH stretching region infrared spectra of low density amorphous solid water and polycrystalline ice Ih. J. Chem. Phys. 69, 3477–3482.

Calvin, W.M., Johnson, R.E., Spencer, J.R., 1996. O_2 on Ganymede: Spectral characteristics and plasma formation mechanisms. Geophys. Res. Lett. 23, 673–676.

Carlson, R.W., Anderson, M.S., Johnson, R.E., Smythe, W.D., Hendrix, A.R., Barth, C.A., Soderblom, L.A., Hansen, G.B., McCord, T.B., Dalton, J.B., Clark, R.N., Shirley, J.H., Ocampo, A.C., Matson, D.L., 1999. Hydrogen peroxide on the surface of Europa. Science 283, 2062–2064.

Chaabouni, H., Schriver-Mazzuoli, L., Schriver, A., 2000. Infrared spectroscopy of neat solid ozone and that of ozone in interaction with amorphous and crystalline water ice. J. Phys. Chem. A 104, 6962–6969.

Cooper, P.D., Moore, M.H., Hudson, R.L., 2006. Infrared detection of HO_2 and HO_3 radicals in water ice. J. Phys. Chem. A 110, 7985–7988.

Cooper, P.D., Kjaergaard, H.G., Langford, V.S., McKinley, A.J., Quickenden, T.I., Schofield, D.P., 2003. Infrared measurements and calculations on $H_2O{\cdot}HO$. J. Am. Chem. Soc. 125, 6048–6049.

Chyba, C.F., 2000. Energy for microbial life on Europa. Nature 403, 381–382; Erratum, Nature 406 (2000) 368.

Ehrenfreund, P., Boogert, A.C.A., Gerakines, P.A., Tielens, A.G.G.M., van Dishoeck, E.F., 1997. Infrared spectroscopy of interstellar apolar ice analogs. Astron. Astrophys. 328, 649–669.

Gomis, O., Satorre, M.A., Strazzulla, G., Leto, G., 2004a. Hydrogen peroxide formation by ion implantation in water ice and its relevance to the Galilean satellites. Planet. Space Sci. 52, 371–378.

Gomis, O., Leto, G., Strazzulla, G., 2004b. Hydrogen peroxide production by ion irradiation of thin water ice films. Astron. Astrophys. 420, 405–410.

Hendrix, A.R., Barth, C.A., Hord, C.W., 1999. Ganymede's ozone-like absorber: Observations by the Galileo ultraviolet spectrometer. J. Geophys. Res. 104, 14169–14178.

Hudgins, D.M., Sandford, S.A., Allamandola, L.J., Tielens, A.G.G.M., 1993. Mid- and far-infrared spectroscopy of ices: Optical constants and integrated absorbances. Astrophys. J. Suppl. 86, 713–870.

Hudson, R.L., Moore, M.H., 1992. A far-IR study of irradiated amorphous ice: An unreported oscillation between amorphous and crystalline phases. J. Phys. Chem. 96, 6500–6504.

Hudson, R.L., Moore, M.H., 1995. Far-IR spectral changes accompanying proton irradiation of solids of astrochemical interest. Rad. Phys. Chem. 45, 779–789.

Johnson, R.E., Jesser, W.A., 1997. O_2/O_3 microatmospheres in the surface of Ganymede. Astrophys. J. 480, L79–L82.

Johnson, R.E., Quickenden, T.I., 1997. Photolysis and radiolysis of water ice on outer Solar System bodies. J. Geophys. Res. 102, 10985–10996.

Johnson, R.E., Luhmann, J.G., Tokar, R.L., Bouhram, M., Berthelier, J.J., Sittler, E.C., Cooper, J.F., Hill, T.W., Crary, F.J., Young, D.T., 2006. Production, ionization and redistribution of Saturn's O_2 ring atmosphere. Icarus 180, 393–402.

Johnson, R.E., Cooper, P.D., Quickenden, T.I., Grieves, G.A., Orlando, T.M., 2005. Production of oxygen by electronically induced dissociations in ice. J. Chem. Phys. 123, 184715.

Laffon, C., Lacombe, S., Bournel, F., Parent, Ph., 2006. Radiation effects in water ice: A near-edge X-ray absorption fine structure study. J. Chem. Phys. 125, 204714.

Loeffler, M.J., Teolis, B.D., Baragiola, R.A., 2006a. Decomposition of solid amorphous hydrogen peroxide by ion irradiation. J. Chem. Phys. 124, 104702.

Loeffler, M.J., Teolis, B.D., Baragiola, R.A., 2006b. A model study of the thermal evolution of astrophysical ices. Astrophys. J. 639, L103–L106.

Loeffler, M.J., Raut, U., Vidal, R.A., Baragiola, R.A., Carlson, R.W., 2006c. Synthesis of hydrogen peroxide in water ice by ion irradiation. Icarus 180, 265–273.

Moore, M.H., Hudson, R.L., 2000. IR detection of H_2O_2 at 80 K in ion-irradiated laboratory ices relevant to Europa. Icarus 145, 282–288.

Nelander, B., 1997. The peroxy radical as hydrogen bond donor and hydrogen bond acceptor: A matrix isolation study. J. Phys. Chem. A 101, 9092–9096.

Nelander, B., Engdahl, A., Svensson, T., 2000. The HOOO radical: A matrix isolation study. Chem. Phys. Lett. 332, 403–408.

Noll, K.S., Johnson, R.E., Lane, A.L., Dominigue, D.L., Weaver, H.A., 1996. Detection of ozone on Ganymede. Science 273, 341–343.

Noll, K.S., Roush, T.L., Cruikshank, D.P., Johnson, R.E., Pendleton, Y.J., 1997. Detection of ozone on Saturn's satellites Rhea and Dione. Nature 388, 45–47.

Orlando, T.M., Sieger, M.T., 2003. The role of electron-stimulated production of O_2 from water ice in the radiation processing of outer Solar System surfaces. Surf. Sci. 528, 1–7.

Palumbo, M.E., 2006. Formation of compact solid water after ion irradiation at 15 K. Astron. Astrophys. 453, 903–909.

Petrik, N.G., Kavetsky, A.G., Kimmel, G.A., 2006. Electron-stimulated production of molecular oxygen in amorphous solid water. J. Phys. Chem. B 110, 2723–2731.

Rowland, B., Fisher, M., Devlin, J.P., 1991. Probing icy surfaces with the dangling-OH-mode absorption: Large ice clusters and microporous amorphous ice. J. Chem. Phys. 95, 1378–1384.

Schriver, L., Barreau, C., Schriver, A., 1990. Infrared spectroscopic and photochemical study of water ozone complexes in solid argon. Chem. Phys. 140, 429–438.

Schriver-Mazzuoli, L., Schriver, A., Lugez, C., Perrin, A., Camy-Peyret, C., Flaud, J.M., 1996. Vibrational spectra of the $^{16}O/^{17}O/^{18}O$ substituted ozone molecule isolated in matrices. J. Mol. Spectrosc. 176, 85–94.

Schriver-Mazzuoli, L., de Saxcé, A., Lugez, C., Camy-Peyret, C., Schriver, A., 1995. Ozone generation through photolysis of an oxygen matrix at 11 K: Fourier transform infrared spectroscopy identification of the $O{\cdots}O_3$ complex and isotopic studies. J. Chem. Phys. 102, 690–701.

Spencer, J.R., Calvin, W.M., Person, M.J., 1995. CCD spectra of the Galilean satellites: Molecular oxygen on Ganymede. J. Geophys. Res. 100, 19049–19056.

Spencer, J.R., Calvin, W.M., 2002. Condensed O_2 on Europa and Callisto. Astrophys. J. 124, 3400–3403.

Zheng, W., Jewitt, D., Kaiser, R.I., 2006a. Formation of hydrogen, oxygen, and hydrogen peroxide in electron-irradiated crystalline water ice. Astrophys. J. 639, 524–548.

Zheng, W., Jewitt, D., Kaiser, R.I., 2006b. Temperature dependence of the formation of hydrogen, oxygen, and hydrogen peroxide in electron-irradiated crystalline water ice. Astrophys. J. 648, 753–761.

Ziegler, J.P., Biersack, J.P., Littmark, U., 1985. The Stopping and Range of Ions in Solids. Pergamon, New York. Also see: http://www.srim.org/.